IOP Publishing and International Atomic Energy Agency Nuclear Fusion
Nucl. Fusion **51** (2011) 083025 (13pp) doi:10.1088/0029-5515/51/8/083025

Trapped particle stability for the kinetic stabilizer

H.L. Berk and J. Pratt[1]

Institute for Fusion Studies, The University of Texas at Austin, Austin, TX 78639, USA

E-mail: hberk@mail.utexas.edu and Jane.Pratt@ipp.mpg.de

Received 4 March 2011, accepted for publication 16 June 2011
Published 14 July 2011
Online at stacks.iop.org/NF/51/083025

Abstract
A kinetically stabilized axially symmetric tandem mirror (KSTM) uses the momentum flux of low-energy, unconfined particles that sample only the outer end-regions of the mirror plugs, where large favourable field-line curvature exists. The window of operation is determined for achieving magnetohydrodynamic (MHD) stability with tolerable energy drain from the kinetic stabilizer. Then MHD stable systems are analysed for stability of the trapped particle mode. This mode is characterized by the detachment of the central-cell plasma from the kinetic-stabilizer region without inducing field-line bending. Stability of the trapped particle mode is sensitive to the electron connection between the stabilizer and the end plug. It is found that the stability condition for the trapped particle mode is more constraining than the stability condition for the MHD mode, and it is challenging to satisfy the required power constraint. Furthermore, a severe power drain may arise from the necessary connection of low-energy electrons in the kinetic stabilizer to the central region.

(Some figures in this article are in colour only in the electronic version)

1. Introduction

The tandem mirror magnetic-fusion confinement system is a nearly cylindrical solenoid terminated by a set of plug cells. These plugs consist of simple axisymmetric mirror fields. The earliest stability theories [1] predicted that symmetric mirror machines, including tandem mirrors, would be MHD unstable; experiments in the 1980s on both TARA [2] and PHAEDRUS [3, 4] tandem mirror facilities confirmed that MHD instability occurs. Recently, a new stability innovation, the kinetic stabilizer, has been proposed to stabilize an axisymmetric tandem mirror. However, the mechanism by which MHD stabilization is achieved in the kinetic stabilizer may make the system susceptible to a rapidly growing trapped particle instability [5]. Here we investigate this possibility.

The kinetic stabilizer is a design proposed by Post [6], inspired by the work of Ryutov and experimental evidence from the gas dynamic trap (GDT), a single mirror experiment at Novosibirsk [7, 8]. Ryutov established theoretically that an otherwise MHD-unstable plasma confined between symmetric mirrors can be stabilized if there is sufficient momentum flux from the effluent plasma on the expanding positive-curvature field-lines outside the mirrors. The momentum flux generalizes the role of the pressure tensor that appears in standard MHD theory. This technique of stabilization was experimentally confirmed using the axisymmetric GDT [9, 10].

[1] Present address: Max-Planck-Institut für Plasmaphysik, 85748 Garching, Germany

The GDT operates in a high-collisionality regime in order to keep the loss-cone full. Ryutov noted that the effect of plasma momentum flux flowing out of the ends of the machine in the positive-curvature expanding-field region outside the mirrors is sufficiently strong to overcome the destabilizing curvature contribution from the central part of the plasma. It has been shown that MHD stability arising from the use of exiting momentum flux can persist up to a moderately high-beta value of $\beta \sim 0.6$.

In the GDT the loss-cone is filled by relatively strong collisions in the central plasma region; with sufficient effluent flow, MHD stability is established. However, in the typical tandem mirror the ends of the machine are designed to confine a long mean-free-path plasma which only produces a weak effluent. Thus there is a negligible momentum flux in the expander region. As a result, the stabilization mechanism designed for the GDT, i.e. stabilization from the momentum flux arising from the effluent plasma, does not simply arise in a tandem mirror of conventional design. The kinetic-stabilizer concept proposes to solve the problem of low effluence using external ion-beams injected axially into the machine. These kinetic-stabilizer ion-beams are injected at small pitch-angles to the magnetic field so that the beam can propagate towards the higher magnetic field and then reflect before reaching the principal confinement region of the mirror plasma. The ion beam then transits out of the machine. While entering and exiting the ends of the machine, the beam forms an unconfined plasma with an enhanced momentum flux in a localized region of favourable curvature.

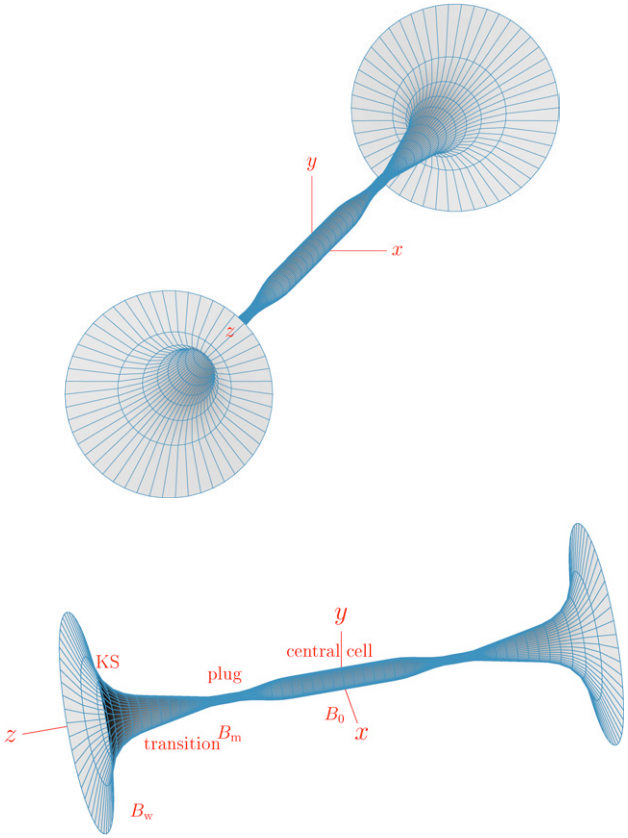

Figure 1. Axisymmetric magnetic flux surfaces in the KSTM.

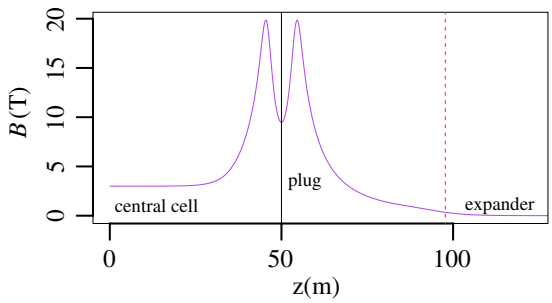

Figure 2. Axial magnetic field B, in the right half of the proposed KSTM reactor. The field-line curvature is negligible to the left of the dashed line. The favourable curvature of the expander region lies to the right of the dashed line. A solid black line marks the centre of the mirror plug.

The proposed kinetically stabilized tandem mirror (KSTM) reactor is a simple axisymmetric tandem mirror. The plasma in the plug regions possesses higher density and energy than the central-cell plasma, producing ambipolar traps in the plugs. The three-dimensional structure of the magnetic flux tube can be viewed in figure 1. Figure 2 provides a schematic diagram of the axial magnetic field of a KSTM; figure 3 provides a conceptual sketch of the density profile associated with the kinetic stabilizer. At the outer wall, on the left-side of figure 3, the magnetic field is at its lowest value $B = B_W$. The density of the beam initially rises in the expander region as we consider regions inward from the wall. The beam can either be focused on a target in the region around $B = B_{ks}$ or unfocused. In the focused case, the density will

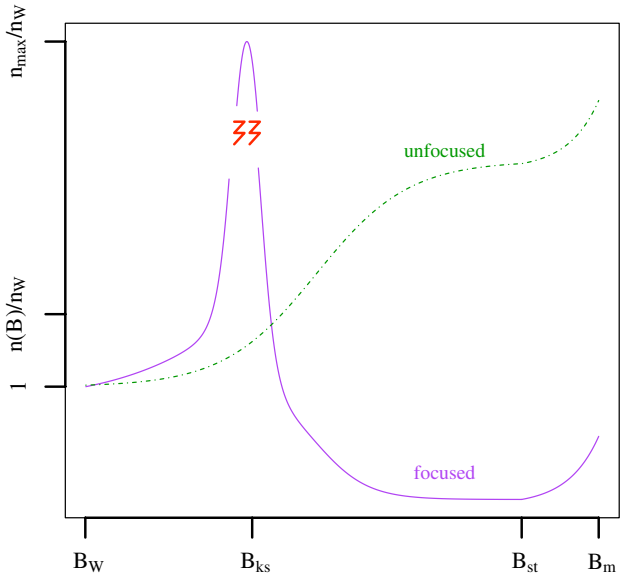

Figure 3. A conceptual sketch of the density in the expander region of the KSTM. The shape of the density at the wall B_W, the entrance to the region of favourable curvature B_{ks}, plateau, stand-off point B_{st}, and the maximum of the plug B_m are shown.

peak steeply around $B = B_{ks}$ and then plummet to a low value just beyond $B = B_{ks}$. The focused kinetic-stabilizer ion beam is designed to reflect around the region of B_{ks} which bounds the region of good curvature that exists between the target and the wall. In the unfocused case the density will continue to rise until most of the kinetic-stabilizer beam has been reflected by the rising magnetic field. The remnant beam that reaches this region possesses a nearly spatially isotropic distribution, which produces a plateau in density. In the plateau region, the density of the unfocused beam is appreciably higher than for a focused beam. The electron temperature between the wall and the plateau region will probably be lower than the ion energy in the injected kinetic stabilizer. However, the temperature of the electrons escaping from the central cell will be from 10 to 100 keV, and thus the ambipolar potential associated with the effluent flux will be extremely high. We expect a transition region around a stand-off position, $B = B_{st}$, where electron temperature transitions from a characteristic temperature of the KS region, to the electron temperature of the core plasma. In this region the plasma density will rise.

The density profile and the relation between density and the electric potential will be discussed further in section 2, where we present the details of the model used for the KSTM. In section 3 we derive MHD stability relations for the KSTM. In section 4 the trapped particle instability is examined in the context of a KSTM and in section 5 we summarize the salient conclusions of this work.

2. KSTM model

2.1. Distribution of ions in the kinetic-stabilizer beam

The kinetic-stabilizer design consists of an ion beam that is injected from outside the machine into the expander region of the tandem mirror where the curvature is positive. The beam

of ions is aligned nearly parallel to the magnetic field. The small pitch-angle of the particles in the beam corresponds to injection of ions with small magnetic-moment-per-unit-mass μ compared with E_0/B (where E_0 is the mean injected-beam-energy-per-unit-mass). We choose a distribution function for the ions in the kinetic-stabilizer beam such that they possess a fixed energy equal to E_0. The magnetic moment is centred around a value μ_0 with a narrow range of magnetic moments $\Delta\mu$. The distribution function, F, is chosen to be

$$F(E,\mu) = \frac{\Gamma'_{\rm ks}}{\pi}\delta(E-E_0)\frac{\Delta\mu}{(\mu-\mu_{\rm T})^2+\Delta\mu^2}. \qquad (1)$$

Here the quantity $\Gamma'_{\rm ks}$ is related to the particle flux per unit magnetic flux $\Gamma_{\rm ks}$ from a single end of the tandem mirror as indicated in (4). The spread in magnetic moments of the kinetic-stabilizer beam is determined by $\Delta\mu$; we use $\mu_{\rm T} = E_0/B_{\rm T}$ where the subscript T refers to the target position; the values of $\Delta\mu$ and $\mu_{\rm T}$ affect the maximum density at the target. We neglect the ion electrostatic potential energy under the assumption that the potential energy is proportional to $T_{\rm eks}$, the electron temperature in the kinetic-stabilizer region. The electron temperature is assumed to be significantly less than the ion beam energy.

We will treat two types of kinetic-stabilizer ion beams. In the case of a focused beam, the beam is focused on a target outside of the plug $\mu_{\rm T}$. For the second type of beam, $\mu_{\rm T} = 0$; this will be referred to as the unfocused case, equivalent to the condition $\mu_{\rm T} \ll \Delta\mu$.

The density and pressure in the outer regions of the KSTM are established by an incoming particle flux at the wall. The subscript W refers to the wall position, i.e. $z = z_{\rm W}$ and $r = r_{\rm W}$. In terms of the distribution, the particle flux at the wall $\pi r_{\rm W}^2 B_{\rm W}\Gamma_{\rm ks}$ is

$$\pi r_{\rm W}^2 B_{\rm W}\Gamma_{\rm ks} = \pi r_{\rm W}^2\int_0^\infty {\rm d}E\int_0^{E/B_{\rm W}} {\rm d}\mu B_{\rm W} F(E,\mu), \qquad (2)$$

$$= r_{\rm W}^2 B_{\rm W}\Gamma'_{\rm ks}\int_0^{E_0/B_{\rm W}} \frac{{\rm d}\mu\ \Delta\mu}{(\mu-\mu_{\rm T})^2+\Delta\mu^2}. \qquad (3)$$

We find

$$\frac{\Gamma_{\rm ks}}{\Gamma'_{\rm ks}} \approx \frac{1}{\pi}\int_0^\infty \frac{{\rm d}\mu\Delta\mu}{(\mu-\mu_{\rm T})^2+\Delta\mu^2} = \frac{1}{2}+\frac{1}{\pi}\tan^{-1}\left(\frac{\mu_{\rm T}}{\Delta\mu}\right)$$
$$\equiv \chi\left(\frac{\mu_{\rm T}}{\Delta\mu}\right). \qquad (4)$$

For the unfocused case, $\mu_{\rm T}/\Delta\mu \ll 1$, $\chi \approx 1/2$, while for the focused case, $\mu_{\rm T}/\Delta\mu \gg 1$, $\chi \approx 1$.

2.2. Density and pressure in the expander due to the kinetic-stabilizer beam

When the effect of the ambipolar potential on the ions is neglected, the density $n(B)$ is

$$n(B) = \sqrt{2}\int_0^\infty {\rm d}E\int_0^{E/B}\frac{{\rm d}\mu B}{\sqrt{E-\mu B}}F(E,\mu). \qquad (5)$$

We define the quantity $x = \mu B/E_0$ and use the distribution function in (1) to express the density integral as

$$n(B) = \frac{\sqrt{2}\Gamma'_{\rm ks}B}{\pi\sqrt{E_0}}\left(\frac{\Delta\mu B}{E_0}\right)$$
$$\times\int_0^1\frac{{\rm d}x}{\sqrt{1-x}}\frac{1}{(x-B/B_{\rm T})^2+(\Delta\mu B/E_0)^2},$$
$$\xrightarrow{\left[1\gg\frac{B}{B_{\rm T}}-1,\ \frac{\Delta\mu B_{\rm T}}{E_0}\ll 1\right]}\ \Gamma'_{\rm ks}B\sqrt{\frac{1}{E_0}}$$
$$\times\frac{\left[\sqrt{\left(1-\frac{B}{B_{\rm T}}\right)^2+\left(\frac{\Delta\mu B}{E_0}\right)^2}+\left(1-\frac{B}{B_{\rm T}}\right)\right]^{1/2}}{\sqrt{\left(1-\frac{B}{B_{\rm T}}\right)^2+\left(\frac{\Delta\mu B}{E_0}\right)^2}},$$
$$\xrightarrow{\left[1-\frac{B}{B_{\rm T}}\gg\frac{\Delta\mu B}{E_0}\right]}\ \Gamma'_{\rm ks}\sqrt{\frac{2}{E_0}}\frac{B}{\sqrt{1-\frac{B}{B_{\rm T}}}}. \qquad (6)$$

The inequality $1 \gg B/B_{\rm T} - 1$ is satisfied for all $B/B_{\rm T} < 1$ when $\Delta\mu B_T/E_0 \ll 1$. The last approximation is also accurate when $|B/B_{\rm T} - 1| \gg \Delta\mu B_{\rm T}/E_0$, but still small.

The inequality $\Delta\mu B/E_0 \gg 1$ determines a region where the density asymptotes to a constant value. We call this region the plateau region, where the density $n_{\rm pla}$ is

$$n_{\rm pla} = \frac{2\sqrt{2}\,\Gamma'_{\rm ks}B_{\rm T}}{\pi\sqrt{E_0}}\frac{\Delta\mu B_{\rm T}}{E_0} \doteq \frac{2}{\pi}\frac{\Delta\mu B_T^2}{E_0 B_{\rm W}}n_{\rm W}\left(1-\frac{B_{\rm W}}{B_{\rm T}}\right)^{1/2}. \qquad (7)$$

Here $n_{\rm W} \equiv n(B_{\rm W})$ is the density at the wall.

For the focused case the density peaks near the target position $B = B_{\rm T}$. At the target the density is given by

$$n(B_{\rm T}) = \frac{\Gamma'_{\rm ks}B_{\rm T}}{\sqrt{2E_0}}\left(\frac{E_0}{\Delta\mu B_{\rm T}}\right)^{1/2}$$
$$= \frac{n_{\rm W}B_{\rm T}}{2B_{\rm W}}\left(\frac{E_0}{\Delta\mu B_{\rm T}}\right)^{1/2}\left(1-\frac{B_{\rm W}}{B_{\rm T}}\right)^{1/2}. \qquad (8)$$

For the unfocused case the density increases monotonically from the wall position to the plateau region. We can relate the density at the wall to the density at the entrance to the region of positive curvature, which we will call the kinetic-stabilizer position, denoted by the subscript ks. Assuming that the axial speed of the beam is small compared with the local thermal spread of its speed, i.e. $\Delta\mu B_{\rm ks}/E_0 \ll 1$, then

$$\frac{n\,(B_{\rm ks})}{n_{\rm W}} \approx \frac{B_{\rm ks}}{B_{\rm W}}\frac{n_{\rm pla}}{n_{\rm W}} \approx \frac{4E_0}{\pi B_{\rm W}\Delta\mu}\left(1-\frac{B_{\rm W}}{B_{\rm T}}\right)^{1/2}. \qquad (9)$$

The plateau region arises when $\Delta\mu B \gg E_0$. By focusing the ion beam to a position $B = B_{\rm T}$, the peak density in the kinetic-stabilizer region is enhanced compared with the unfocused case by an approximate factor of $(E_0/\Delta\mu B_{\rm T})^{1/2}$. In the plateau region, the density of the unfocused case is larger than the focused case by a factor of $(E_0/\Delta\mu B_{\rm T})^2$.

In magnetized mirror-confined plasmas the pressure is typically anisotropic with different values for the pressures $p_\perp$, and $p_\parallel$ respectively. The mass of ions in the kinetic-stabilizer beam is taken as $m_{\rm i}$. For our choice of distribution function,

the pressures are

$$p(B) = p_\parallel(B) + p_\perp(B) = n(B)m_i E_0 + p_\parallel(B)/2, \tag{10}$$

$$p_\parallel(B) = 2\sqrt{2}\, m_i \int_0^\infty \mathrm{d}E \int_0^{E/B} \mathrm{d}\mu B\sqrt{E-\mu B}\; F(E,\mu), \tag{11}$$

$$p_\perp(B) = 2\, m_i \int_0^\infty \mathrm{d}E \int_0^{E/B} \frac{\mathrm{d}\mu\mu B^2}{\sqrt{2(E-\mu B)}} F(E,\mu) = n(B)m_i E_0 - \frac{p_\parallel(B)}{2}. \tag{12}$$

The integral for $p_\parallel(B)$ is

$$p_\parallel(B) = \frac{2\sqrt{2}}{\pi} m_i \Gamma'_{ks}\, B\sqrt{E_0} \int_0^1 \frac{\mathrm{d}x\, \frac{\Delta\mu B}{E_0}\sqrt{1-x}}{\left(x-\frac{B}{B_T}\right)^2 + \left(\frac{\Delta\mu B}{E_0}\right)^2}, \tag{13}$$

$$\overset{[\Delta\mu=0]}{\longrightarrow} 2m_i\Gamma'_{ks}\sqrt{2E_0}\left(1-\frac{B}{B_T}\right)^{1/2}\theta\left(1-\frac{B}{B_T}\right), \tag{14}$$

where $\theta(x)$ is the Heaviside step function. For the focused case where $\Delta\mu B_T/E_0 \ll 1$, the perpendicular pressure peaks near the target, $B \approx B_T$, and is approximately

$$p_\perp(B) \cong m_i E_0 n(B), \tag{15}$$

while the parallel pressure remains small. Thus the ratio of pressure at the target to that at the wall is proportional to the ratio of magnetic fields at these positions

$$\frac{p_\perp(B_T)}{p_\perp(B_W)} \sim \frac{B_T}{B_W}\left(\frac{E_0}{\Delta\mu B_T}\right)^{1/2}. \tag{16}$$

In the plateau region the pressure is isotropic and constant with

$$p_\perp(B) = p_\parallel(B) = \frac{4}{3}\sqrt{2}\,\pi\, \frac{\Gamma'_{ks}}{\sqrt{E_0}} \frac{\Delta\mu B_T^2}{\left[1+\left(\frac{\Delta\mu B_T}{E_0}\right)^2\right]}. \tag{17}$$

When $\Delta\mu B_T \gg E_0$, which is the definition of the unfocused case, the pressure in the plateau region is $p_\perp(B) = p_\parallel(B) = \sqrt{2}\pi(4/3)(\Gamma'_{ks}/\sqrt{E_0})(E_0^2/\Delta\mu)$. This pressure is larger than the focused case by a factor of $(E_0/\Delta\mu B_T)^2$.

3. KSTM MHD stability relations

During steady-state operation, the power P required to sustain the power drain of a single-pass kinetic-stabilizer beam is

$$P = 4(1-\nu)\pi m_i E_0 \Gamma_{ks}\psi_0, \tag{18}$$

where ν is the efficiency of recovery the beam power energy by direct conversion [11]. The expression for power in (18) also uses the magnetic flux $\psi_0 = \frac{1}{2}B_0 r_0^2$ at the centre of the central cell of the tandem mirror. The limiting condition for achieving break-even for reactor engineering is that the power drain from the kinetic-stabilizer beams should not exceed the alpha particle energy production rate of the central-cell by more than some factor η'. We take $\eta' = 1$ in our calculations. Hence we have

$$\eta\pi r_0^2 m_i E_0 B_0 \Gamma_{ks} < \frac{3\pi r_0^2 L_c T_c n_c^2}{2\langle n\tau\rangle_{fus}}, \tag{19}$$

where we define $\eta = \eta'/(1-\nu)$. If $\nu = 0.8$, a value perhaps possible with direct conversion [11], the largest value possible for η would be 5. The temperature in (19) is a sum of electron and ion temperatures $T_c = T_{ec} + T_{ic}$ and the subscript c refers to the central cell. The Lawson criterion $\langle n\tau\rangle_{fus} = 2\times 10^{20}\,\mathrm{m}^{-3}$ should hold for our model KSTM. For MHD stability, we require

$$\int_{ks} \mathrm{d}z\,(p_\parallel + p_\perp)\, r^3 \frac{\mathrm{d}^2 r}{\mathrm{d}z^2} > \int_{\text{plug + central cell}} \mathrm{d}z\,(p_\parallel + p_\perp)\, r^3 \frac{\mathrm{d}^2 r}{\mathrm{d}z^2}. \tag{20}$$

To evaluate the MHD stability criterion in (20) we constrain the field-line radius $r(z)$ to have as large as possible variation within the kinetic-stabilizer region that is compatible with the paraxial approximation. Thus, field-line radius $r(z)$ must satisfy

$$r\frac{\mathrm{d}^2 r(z)}{\mathrm{d}z^2} = r(z)\frac{\mathrm{d}}{\mathrm{d}r}\left(\frac{\mathrm{d}r(z)}{\mathrm{d}z}\right)^2 = \frac{\sigma_p}{2}. \tag{21}$$

We will refer to (21) as the marginal paraxial constraint. For optimal stability, the constant σ_p in the the marginal paraxial constraint should be chosen to maximize the integrand on the left-hand side of (20), subject to the validity of the paraxial approximation for the field-line curvature; in this work we use $\sigma_p = 1$ while acknowledging that additional study is needed to determine an optimal value.

Solving (21) for $r(z)$ yields

$$z - z_{ks} = \int_{r_{ks}}^{r} \frac{\mathrm{d}r}{\left[\sigma_p \ln\left(\frac{r}{r_{ks}}\right) + \left(\frac{\mathrm{d}r(z_{ks})}{\mathrm{d}z}\right)^2\right]^{1/2}} \leqslant \frac{r_W}{\sqrt{\sigma_p}} \int_{r_{ks}/r_W}^{r/r_W} \frac{\mathrm{d}y}{\left[\ln\left(\frac{r_W}{r_{ks}}y\right)\right]^{1/2}}. \tag{22}$$

When $\mathrm{d}r(z_{ks})/\mathrm{d}z = 0$, the inequality in (22) is an equality. Since the choice of $\mathrm{d}r(z_{ks})/\mathrm{d}z = 0$ maximizes the favourable MHD response, this field-line slope is used in our model for KSTM field-lines.

3.1. Stability integral in the plug

We model the field-line radius in the plug region with the form

$$r(z) = r_{mxp}\left(\frac{1+x_{pl}}{2} + \frac{1-x_{pl}}{2}\cos\left(\frac{2\pi(z-L_c)}{L_{pl}}\right)\right), \tag{23}$$

where $x_{pl} = r_{mnp}/r_{mxp}$. The radii r_{mxp} and r_{mnp} are the maximum and minimum radii of the plug region, and $0 < |z - L_c| < L_{pl}$. We define the composite pressure $p = (p_\perp + p_\parallel)/2$. We also define

$$\overline{p}_{pl} = \frac{1}{2L_{pl}}\int_{L_c}^{L_c+L_{pl}} \mathrm{d}z\,(p_\perp + p_\parallel) = \frac{1}{2L_{pl}}\int_{pl} \mathrm{d}z\; p. \tag{24}$$

The dimensionless plasma parameter in this region is defined $\overline{\beta}_{pl} = 2\mu_0\overline{p}_{pl}/B^2_{mnp}$, where B_{mnp} is the magnetic field at the minimum field-line radius in the plug region. We define I_{pl} to

be the stability integral over the plug region for the particular magnetic field assumed in (23). Thus we need to evaluate

$$I_{\rm pl} = -2\int_{\rm pl} {\rm d}z \overline{p}_{\rm pl} r^3 \frac{{\rm d}^2 r}{{\rm d}z^2}. \tag{25}$$

We indicate an approximation of $I_{\rm pl}$ with a prime. We evaluate $I'_{\rm pl}$, as the approximate stability integral $I_{\rm pl}$ when the pressure is taken as isotropic in the plug with a pressure $\overline{p}_{\rm pl}$. We obtain

$$I'_{\rm pl} = \frac{3\pi^2 \overline{p}_{\rm pl}}{4L_{\rm pl}} r_{\rm mxp}^4 \left(1 - x_{\rm pl}^2\right)^2 \left(1 + \frac{1}{4}\left(\frac{1 - x_{\rm pl}}{1 + x_{\rm pl}}\right)^2\right). \tag{26}$$

In this expression we have used the paraxial approximation for the magnetic flux $r_{\rm mxp}^2 B_{\rm mnp} \approx B_0 r_0^2$. For simplicity we have neglected the small factor $(1 - x_{\rm pl})^2/(2(1 + x_{\rm pl}))^2$ in the estimate $I'_{\rm pl}$. We define $\alpha_{\rm pl}$ as a dimensionless, order-unity parameter that is the ratio of the exact to the estimated value of the stability integral

$$\alpha_{\rm pl} = I_{\rm pl}/I'_{\rm pl}. \tag{27}$$

The factor $\alpha_{\rm pl}$ may be less than unity (e.g. due to the inclusion of compressibility effects in the plug cell and improved design of the plug, etc) and such improvement gives some flexibility in estimating a window of operation for the KSTM.

The contribution to MHD stability from the central cell must also be considered and is treated in the same way as the plug. We use a shape of the same form as the plug region described in (23), and central-cell parameters $r_{\rm mxp} \to r_0$, $L_{\rm pl} \to 2L_{\rm c}$, $z - L_{\rm c} \to z$, $x_{\rm pl} \to x_{\rm c} = r_0/r_{\rm mn}$. Thus

$$r(z) = r_0\left(\frac{1 + x_{\rm c}}{2} + \frac{1 - x_{\rm c}}{2}\cos\left(\frac{2\pi z}{L_{\rm c}}\right)\right). \tag{28}$$

The central-cell stability contribution will be used below.

3.2. Stability integral in the expander region

For our KSTM model there is no contribution to the stability integral from the intermediate region between the outlet of the plug (defined by the maximum of the magnetic field) and the beginning of the positive-curvature kinetic-stabilizer region at $z = z_{\rm ks}$. The stability contribution of this intermediate expander region would vanish if either ${\rm d}^2 r/{\rm d}z^2$ or the kinetic pressure were negligible.

The MHD contribution of the stability drive integral from the expander region is

$$I_{\rm ks} = \int_{z_{\rm ks}}^{z_{\rm w}} {\rm d}z \left(p_\parallel + p_\perp\right) r^3 \kappa. \tag{29}$$

In this expression κ is the field-line curvature,

$$\kappa = \frac{\frac{{\rm d}^2 r}{{\rm d}z^2}}{\left[1 + \left(\frac{{\rm d}r}{{\rm d}z}\right)^2\right]^{3/2}} \approx \frac{{\rm d}^2 r}{{\rm d}z^2}. \tag{30}$$

The paraxial approximation of the curvature is given in the right-most term of (30).

To establish a base-case for scaling our results, we consider the unfocused kinetic-stabilizer beam ($\Delta\mu = 0$), and use the paraxial approximation for the curvature. Using the fact that magnetic flux is conserved, $Br^2 = B_0 r_0^2$, the expressions for the pressures from (11) and (12), and the solution $r(z)$ from (22), we find

$$\begin{aligned} I_{\rm ks} &= \int_{z_{\rm ks}}^{z_{\rm w}} {\rm d}z \left(p_\parallel + p_\perp\right)\Big|_{\Delta\mu=0} r^3 \frac{{\rm d}^2 r}{{\rm d}z^2} \\ &= 2m_{\rm i}\sqrt{2\sigma_{\rm p} E_0}\; B_0 r_0^2 \Gamma'_{\rm ks} r_{\rm w} \int_{r_{\rm ks}/r_{\rm w}}^1 \frac{{\rm d}y}{\sqrt{\ln\left(\frac{r_{\rm w}}{r_{\rm ks}} y\right)}}, \end{aligned} \tag{31}$$

where we have used the slope ${\rm d}r_{\rm ks}/{\rm d}z = 0$. We approximate the stability integral in the expander region as

$$I'_{\rm ks} = 2m_{\rm i}\sqrt{\sigma_{\rm p} 2E_0}\; B_0 r_0^2 \Gamma'_{\rm ks} r_{\rm w}. \tag{32}$$

We define the ratio of the exact to the approximate stability integrals

$$\alpha_{\rm ks} = \frac{I_{\rm ks}}{I'_{\rm ks}}. \tag{33}$$

In (31) the use of the paraxial approximation for the curvature allows $I_{\rm ks}$ to be made arbitrarily large by increasing $\sigma_{\rm p}$. However, as $\sigma_{\rm p}$ increases, the paraxial approximation is eventually violated. To verify consistency between $I_{\rm ks}$ and the approximate paraxial approximation, we choose $\sigma_{\rm p} = 1$ and compare the results for the non-paraxial expression for the field-line curvature with the results of the paraxial approximation. We use the paraxial solution for z from (22) and the more accurate form of the curvature κ to calculate the integral

$$\begin{aligned} &\frac{\sigma_{\rm p}}{r_{\rm w}} \int_{z_{\rm ks}}^{z_{\rm w}} \frac{{\rm d}z r \kappa}{\left(1 + \left(\frac{{\rm d}r}{{\rm d}z}\right)^2\right)^{3/2}} \\ &\quad = \int_{r_{\rm ks}/r_{\rm w}}^1 \frac{{\rm d}y}{\sqrt{\ln\left(\frac{r_{\rm w}}{r_{\rm ks}} y\right)}} \frac{1}{\left(1 + \sigma_{\rm p} \ln\left(\frac{r_{\rm w}}{r_{\rm ks}} y\right)\right)^{3/2}}. \end{aligned} \tag{34}$$

For the unfocused case (31) becomes

$$\begin{aligned} I_{\rm ks\,0} &\equiv \int_{z_{\rm ks}}^{z_{\rm w}} {\rm d}z r^2 \kappa \left(p_\parallel + p_\perp\right)\Big|_{\Delta\mu=0} \\ &= I'_{\rm ks} \int_{r_{\rm ks}/r_{\rm w}}^1 \frac{{\rm d}y}{\sqrt{\ln\left(\frac{r_{\rm w}}{r_{\rm ks}} y\right)}\left(1 + \sigma_{\rm p} \ln\left(\frac{r_{\rm w}}{r_{\rm ks}} y\right)\right)^{3/2}}. \end{aligned} \tag{35}$$

Figure 4 shows the comparative accuracy of the paraxial approximation and the more accurate non-paraxial curvature for $\alpha_{\rm ks} = I_{\rm ks}/I'_{\rm ks}$ as a function of $x = r_{\rm ks}/r_{\rm w}$. The maxima are $\alpha_{\rm ks} = 1.08$ for $x_{\rm ks} = 0.43$ for the paraxial form and $\alpha_{\rm ks} = 0.815$ for $x_{\rm ks} = 0.63$ for the non-paraxial form. There is some quantitative discrepancy, which indicates that $\sigma_{\rm p} = 1$ may be the largest value that can be used in the expression for $I_{\rm ks}$ to give reliable results.

Larger values of $I_{\rm ks}$ can be obtained by focusing the beam so that the target is at the kinetic-stabilizer point $B_{\rm T} = B_{\rm ks}$. When the beam is focused on this location, a logarithmic

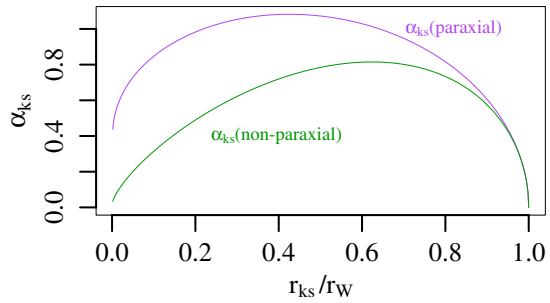

Figure 4. The quantity $\alpha_{ks} = I_{ks}/I'_{ks}$ evaluated for an unfocused kinetic-stabilizer beam from (35) using $\sigma_p = 1$.

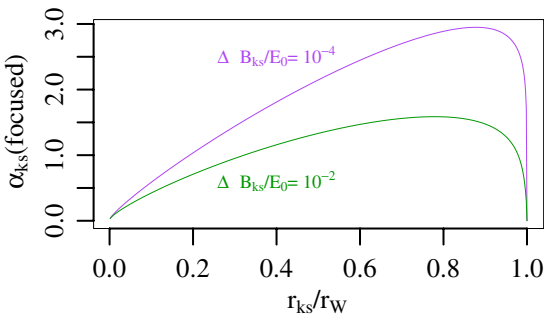

Figure 5. The quantity $\alpha_{ks} = I_{ks}/I'_{ks}$ in the focused case (31), evaluated at two different beam widths.

divergence arises in I_{ks}, producing arbitrarily strong MHD stabilization. For a beam with thermal spread (finite $\Delta\mu$), the magnitude of the stability integral I_{ks} is bounded. To evaluate the stability integral in this case we use an approximate form for the pressure:

$$\frac{2p}{Bm_i\sqrt{E_0}\,\Gamma'_{ks}} = \frac{\left[\sqrt{\left(1-\frac{B}{B_T}\right)^2+\left(\frac{\Delta\mu B}{E_0}\right)^2}+1-\frac{B}{B_T}\right]^{1/2}}{\sqrt{\left(1-\frac{B}{B_T}\right)^2+\left(\frac{\Delta\mu B}{E_0}\right)^2}} + \sqrt{1-\frac{B}{B_T}}\,\theta\left(1-\frac{B}{B_T}\right). \tag{36}$$

This is valid if $1 \gg B/B_T - 1$, a condition that is always satisfied when the right-hand side is negative and $\Delta\mu B_T/E_0 \ll 1$. Again using the condition that magnetic flux is conserved, so $B/B_{ks} = (r_{ks}/r)^2$, and setting the target position T at the kinetic-stabilizer position KS, we obtain a stability integral $I_{fo} \equiv I_{ks}$ for the focused case

$$I_{fo} = I'_{ks}\, g\left(\frac{r_{ks}}{r_W}, \frac{\Delta\mu B_{ks}}{E_0}\right), \tag{37}$$

$$g(y,\epsilon) = \int_y^1 \frac{dx}{\sqrt{\ln\left(\frac{x}{y}\right)}\left(1+\sigma_p \ln\left(\frac{x}{y}\right)\right)^{3/2}} \times\left[\theta\left(1-\left(\frac{y}{x}\right)^2\right)\sqrt{2\left(1-\left(\frac{y}{x}\right)^2\right)} + \frac{\left(\sqrt{\left(1-\left(\frac{y}{x}\right)^2\right)^2+\left(\epsilon\left(\frac{y}{x}\right)^2\right)^2}+\sqrt{1-\left(\frac{y}{x}\right)^2}\right)^{1/2}}{\sqrt{\left(1-\left(\frac{y}{x}\right)^2\right)^2+\left(\epsilon\left(\frac{y}{x}\right)^2\right)^2}}\right]. \tag{38}$$

A plot of $\alpha_{ks} = I'_{fo}/I'_{ks}$ as a function of r_{ks}/r_W is shown in figure 5 for the focused case, where $(\Delta\mu B_{ks}/E_0 = 10^{-2}, 10^{-4})$. As $\Delta\mu B_{ks}/E_0$ decreases, the optimal MHD response is found closer to the wall; at small $\Delta\mu B_{ks}/E_0$, the value of this optimal response is given by $0.2 + 0.7\log_{10}(E_0/\Delta\mu B_{ks})$. For $\Delta\mu B_{ks}/E_0 = 10^{-4}$ this leads to $\alpha_{ks} \approx 3$.

3.3. Operating regime scaling laws

For our machine to be stable we require $M_{ks} \equiv (I_{pl}+I_c)/I_{ks} < 1$ or

$$1 > M_{ks} = \frac{3\pi^2 r_0^2\left[\alpha_{pl}\overline{p}_{pl}\frac{\left(1-x_{pl}^2\right)^2}{L_{pl}}\left(\frac{r_{mxp}^2}{r_0^2}\right)^2+\alpha_c n_c T_c\frac{\left(1-x_c^2\right)^2}{4L_c}\right]}{8\alpha_{ks}\sqrt{\sigma_p 2E_0}\, r_W m_i B_0\Gamma'_{ks}} = \frac{3\pi^2 r_0^2\, B_0^2}{16\alpha_{ks}\, r_W\sqrt{2E_0\sigma_p}\,\mu_0 m_i B_0\Gamma'_{ks}} \times\left[\frac{\alpha_{pl}\,\overline{\beta}_{pl}}{L_{pl}}\left(1-x_{pl}^2\right)^2+\alpha_c\frac{\overline{\beta}_c\left(1-x_c^2\right)^2}{4L_c}\right], \tag{39}$$

where $x_c = r_0/r_{mxp}$, $T_c = T_{ec}+T_{ic}$. We shall call M_{ks} the MHD marginality parameter. The stability condition of (39) uses the approximations for the stability drive integrals in the plug given by (26) and in the kinetic-stabilizer region given by (31). The MHD drive from the central cell uses the same functional forms for the magnetic field's axial variation as the plug region, and employs the appropriate changes in lengths and mirror ratio. The total length of the central-cell region is $2L_c$. In this stability criterion the central-cell drive is integrated over only half of the central cell. The quantity α_c is the ratio of the actual MHD drive to the scaled MHD drive in the central cell.

From the power-balance relation (19) we find

$$\frac{\eta 3\pi r_0^2 L_c T_c n_c^2}{2\langle n\tau\rangle_{fus}\,\chi\left(\frac{\mu_T}{\Delta\mu}\right)} > \pi r_0^2 E_0 B_0 m_i \Gamma'_{ks} > \frac{3\pi^3\sqrt{2E_0}\, B_0^2 r_0^4}{32\sqrt{\sigma_p}\,\alpha_{ks} r_W\mu_0}\left(\frac{\alpha_{pl}\overline{\beta}_{pl}}{L_{pl}}(1-x_{pl}^2)^2+\frac{\alpha_c\overline{\beta}_c(1-x_c^2)^2}{4L_c}\right). \tag{40}$$

Thus the condition that the system be MHD stable with an acceptable energy loss from the kinetic-stabilizer beam is

$$\frac{r_W}{r_0} = \sqrt{\frac{B_0}{B_W}} > \frac{\pi^2 r_0}{80\sqrt{\sigma_p} n_c L_c L_{pl}}\frac{\langle n\tau\rangle_{fus}\sqrt{2E_0}\,\chi\left(\frac{\mu_T}{\Delta\mu}\right)}{\alpha_{ks}\eta} \times\left(10\alpha_{pl}\left(1-x_{pl}^2\right)^2\frac{\overline{\beta}_{pl}}{\overline{\beta}_c}+\frac{10}{4}\alpha_c\frac{L_{pl}}{L_c}\left(1-x_c^2\right)^2\right). \tag{41}$$

The plasma beta is $\beta_c = nT_c 2\mu_0/B_0^2$. We use

$$n_c^{-1}(m^{-3}) = 4.5\times10^{-21}\frac{T_c(100\,keV)}{\beta_c}\left(\frac{3}{B_0(T)}\right)^2. \tag{42}$$

Normalizing (42) to a reference parameter of approximately 100 MW fusion power production, we find

$$\frac{r_W}{r_0}=\sqrt{\frac{B_0}{B_W}}>70.\frac{\lambda_c\sqrt{E_0(\mathrm{keV})}}{r_0(\mathrm{m})}\left(\frac{T_c(100\,\mathrm{keV})}{\beta_c}\right)\left(\frac{3}{B_0(\mathrm{T})}\right)^2. \tag{43}$$

Here λ_c is a dimensionless parameter that characterizes the machine

$$\lambda_c\equiv\frac{\chi\left(\frac{\mu_T}{\Delta\mu}\right)}{\alpha_{ks}\eta\sqrt{\sigma_p}}\left(\frac{100r_0}{L_c}\right)\left(\frac{5r_0}{L_{pl}}\right)\left(\frac{2}{m_i(a)}\right)^{1/2} \times\left(10\alpha_{pl}\left(1-x_{pl}^2\right)^2\frac{\overline{\beta}_{pl}}{\overline{\beta}_c}+2.50\alpha_c\frac{L_{pl}}{L_c}\left(1-x_c^2\right)^2\right). \tag{44}$$

The injected ion mass $m_i(a)$ in the kinetic-stabilizer beam is in atomic units so that $m_i=2$ for deuterium. The Lawson number $\langle n\tau\rangle_{fus}=2\times10^{20}\,\mathrm{m}^{-3}$ is used to characterize the alpha particle power production; the terms in each of the parentheses is estimated to be order unity and thus $\lambda_c\simeq1$ is a characteristic estimate.

The scaling law (43) indicates whether a system with a given set of parameters can be MHD stable with an acceptable energy loss from the kinetic-stabilizer beam. We choose a reasonable set of parameters to test the MHD stability:

$$B_0(\mathrm{T})=3\mathrm{T},\qquad T_c(100)=100\,\mathrm{keV},\qquad r_0=\frac{1}{\sqrt{3}}\,\mathrm{m},$$
$$L_c=\frac{100}{\sqrt{3}}\,\mathrm{m},\qquad L_{pl}=5r_0=\frac{5}{\sqrt{3}}\,\mathrm{m},$$
$$\overline{\beta}_{pl}=\frac{\beta_c}{5}=\alpha_{ks}=\alpha_c=2\alpha_{pl}=1,$$
$$x_{pl}^2=0.5,\quad x_c^2=0.1,\quad m_i(a)=2,\quad \eta=1. \tag{45}$$

With this choice of parameters we find $\lambda_c=0.175$. We find it necessary to have $B_W<66\,\mathrm{G}$ when $E_0=1\,\mathrm{keV}$ or $B_W<660\,\mathrm{G}$ when $E_0=100\,\mathrm{eV}$. For the parameters in (45) the instability drive of the central cell is 0.4 times the drive from the plug. If the drive from the plug could be reduced or eliminated, (e.g. the plug drive could be neutralized if the particle species in the plug were sufficiently energetic [12]), the drive in the central cell alone would require $B_W<7.9\,\beta_c^2 10^2\,\mathrm{G}$ for $E_0=1\,\mathrm{keV}$ (or $0.79\,\beta_c^2\,\mathrm{T}$ if $E_0=100\,\mathrm{eV}$).

The use of high-current beams are technologically easier to establish at higher energy. However, the energy of the beam does not scale well with the constraint expressed in (41) that the MHD system be stable with an acceptable energy loss from the kinetic-stabilizer beam. This constraint is mitigated if direct conversion of the beam energy is used [11]; direct conversion allows for an increased value of the break-even factor η, with the maximum possible beam energy increasing by a factor of η^2 as follows from (44). Thus, the kinetic-stabilizer beam energy choices of 100 keV and 10 keV would require $B_W<16.5\,\mathrm{G}$ and $B_W<165\,\mathrm{kG}$ respectively, which are reasonable design conditions. Detailed improvements in design that increase λ_c would allow the energy of the kinetic-stabilizer beam to be increased by a factor λ_c^2, with all other parameters fixed.

In summary we find that an expander whose magnetic field at the wall could be as large as the order of several 100 G would enable MHD stability to be achieved by kinetic-stabilizer beams of several hundred eV, in combination with 3 T central-cell magnetic field and $\alpha_{pl}\approx0.5$. The detailed scaling is indicated in (43) and (44).

3.4. Beta limitation and adiabaticity limits

An additional facet of the kinetic-stabilizer ion plasma beta should be considered. When β becomes larger than unity, typically the field-lines cannot collimate the plasma because self-consistent effects drive the plasma across field-lines [13]. For the injected kinetic-stabilizer ions, the local $\beta_{ks}=2\mu_0p/B^2$ must be less than unity along the imposed field-lines. From (36) we find that in the kinetic-stabilizer region

$$\beta_{ks}=\frac{2\mu_0p}{B^2}=\frac{\mu_0}{B}m_i\sqrt{E_0}\Gamma'_{ks}\left[\frac{[[(1-b_T)^2+\epsilon_{ks}^2b_{ks}^2]^{1/2}+1-b_T]^{1/2}}{[(1-b_T)^2+\epsilon_{ks}^2b_{ks}^2]^{1/2}}+2(1-b_T)^{1/2}\right]. \tag{46}$$

Expressing Γ'_{ks} in terms of β_{ks}, we find that the MHD stability condition from (39) and the expression for β_{ks} in (46) can be expressed as

$$1>M_{ks}\equiv\frac{3\pi^2}{64\sqrt{2}}\frac{r_0^2}{r_W^2}\frac{B_0}{B\sqrt{\sigma_p}}\frac{r_W}{L_c}\frac{\alpha_c\overline{\beta}_c}{\beta_{ks}}(1-x_c^2)^2 \times\left[1+\frac{4\alpha_{pl}}{\alpha_c}\frac{L_c}{L_{pl}}\frac{\beta_{pl}}{\beta_c}\frac{(1-x_{pl}^2)^2}{(1-x_c^2)^2}\right] \times\left[\frac{[[(1-b_T)^2+\epsilon_{ks}^2b_{ks}^2]^{1/2}+1-b_T]^{1/2}}{[(1-b_T)^2+\epsilon_{ks}^2b_{ks}^2]^{1/2}}+\sqrt{2(1-b_T)}\right]. \tag{47}$$

Here we again use the conservation of flux $(r_0^2/r_W^2)(B_0/B)=(B_W/B)$. If the inequality has to be satisfied at every position, (47) becomes

$$1>M_{ks}>\frac{0.33\alpha_c}{\sqrt{\sigma_p}}(1-x_c^2)^2\beta_c g M_X, \tag{48}$$

$$g=\left[1+\frac{4\alpha_{pl}}{\alpha_c}\frac{L_c}{L_{pl}}\frac{\beta_{pl}}{\beta_c}\frac{(1-x_{pl}^2)^2}{(1-x_c^2)^2}\right]. \tag{49}$$

Here the expression M_X is the maximum with respect to B of the function

$$M_X=\mathrm{Max}\left[\frac{B_W}{B}\left[\frac{[[(1-b_T)^2+\epsilon_{ks}^2b_{ks}^2]^{1/2}+1-b_T]^{1/2}}{[(1-b_T)^2+\epsilon_{ks}^2b_{ks}^2]^{1/2}}+\sqrt{2(1-b_T)}\right]\right]. \tag{50}$$

For the unfocused case where $b_T=0$ (also nearly applicable for the focused case if $\epsilon_{ks}B_{ks}^2/B_W^2\geqslant1$), the maximum of this function occurs at $B=B_W$, so $M_X=2\sqrt{2}\sqrt{1-B_W/B_{ks}}$. For the focused case, when $\epsilon_{ks}B_{ks}^2/B_W^2\ll1$ the maximum occurs when $b_{ks}=b_T=1-\epsilon_{ks}/\sqrt{3}$, yielding $M_X=1.26(B_W/B_{ks})(1/\sqrt{\epsilon_{ks}})$.

The best MHD condition is achieved by making M_{ks} as small as possible subject to the condition that β_{ks} always remain less than unity. To fulfil MHD expectations and the $\beta_{ks}<1$ condition limits the allowable range for M_{ks} in the unfocused case (or a focused case where $\Delta\mu B_{ks}/E_0>1$) to

$$1>M_{ks}=0.95\sqrt{1-B_W/B_T}\frac{\alpha_c\beta_c}{\sqrt{\sigma_p}}g. \tag{51}$$

For the focused case the permitted range of operation for M_{ks} is

$$1 > M_{ks} \geqslant 0.4 \frac{B_W}{B_{ks}} \frac{\alpha_c \beta_c}{\sqrt{\sigma_p} \epsilon_{ks}^{1/2}} g. \quad (52)$$

Thus the condition that the beta value of the kinetic-stabilizer beam be less than unity may limit the utility of obtaining enhanced MHD stabilization by focusing the beam at $B = B_T$ because the inequality in (52) could be violated for small ϵ_{ks}.

Another possible limitation to the KSTM is that the upper ratio of $B_0/B_W = r_W^2/r_0^2$ must satisfy the particle orbit adiabaticity condition. The ion parallel velocity must be significantly larger than the curvature drift velocity, requiring that

$$\sqrt{2E_0}\,\sigma_{ad} > \frac{2E_0}{\omega_{ci}(z_W)} \frac{d^2 r(z_W)}{dz^2} = \sigma_p \frac{E_0}{\omega_{ci}(z_W) r_W}, \quad (53)$$

where $\sigma_{ad} \sim 1$ is a constant associated with the adiabaticity. We find

$$B_W(\text{gauss}) \geqslant \frac{0.2E(\text{keV})}{B_0(T) r_0^2(\text{m})} \left(\frac{\sigma_p}{\sigma_{ad}}\right)^2 \left(\frac{m_i(a)}{2}\right). \quad (54)$$

For a 100 MW reactor where $B_0(T) r_0^2(m) \cong 1\,\text{T}\,\text{m}^2$, the adiabaticity constraint does not impose a serious restriction on the choice of design parameters.

4. Trapped particle instability

Now let us consider the influence of the trapped particle mode to the stability of the KSTM. The crucial aspect to establish stability of the trapped particle mode is to have enough electrons that communicate between the central-cell region and kinetic-stabilizer region. To determine if stabilization of the fast-growing trapped particle mode is possible, we estimate the fraction of electrons in the kinetic-stabilizer region that need to reflect back into the central plasma [14].

To obtain a reasonable estimate we need to describe the structure of the potential well in the region outside of the plugs. Immediately outside of the MHD destabilizing plug (shown on the right-hand side of figure 6) an ambipolar potential energy of electrons exists, $\Psi(B) = -|e|\Phi(B)$ (with the choice $\Phi_W = 0$). This ambipolar potential forms in the region between the wall and plugs, preventing all but the most energetic electrons from escaping. The effective potential acting on electrons is $U_{\text{eff}}(B) = \Psi(B) + \mu B$. Due to the opposite sign of their electric charge, the ambipolar potential forces an immediate escape of any ions that reach the expander region beyond the plug.

In the region labelled R1 in figure 6, the escaping ions experience an increase in kinetic energy, $E = T_{ic} + \kappa T_{e0}$ that is several times the central-cell electron temperature, with $\kappa \simeq 5$. The ions in this escaping beam are moving nearly parallel to the magnetic field. We assume that there is a rapid transition around a *stand-off region* where $B = B_{st}$. At the stand-off region there is a transition in the ambipolar potential; towards the central-cell region (to the right of B_{st} in figure 6). The ambipolar potential energy varies on the scale of the central-cell electron temperature. Towards the kinetic-stabilizer region (to the left of B_{st} in figure 6) the ambipolar potential tracks with

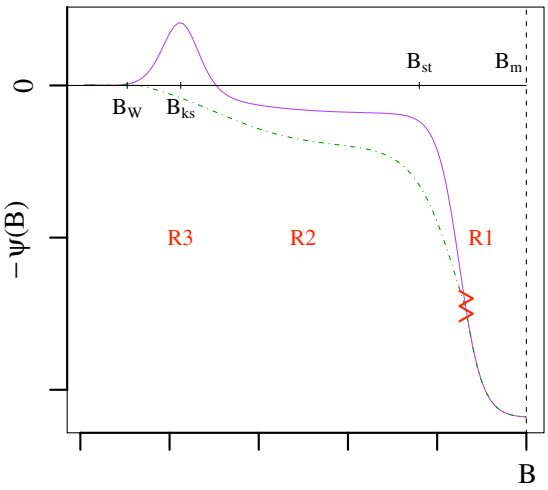

Figure 6. Schematic diagram of the negative of the electrostatic potential energy felt by the electrons for the focused (solid) and unfocused (dashed) cases. In region R1, the ambipolar potential is determined by the electron temperature of the tandem-mirror-confined plasma. Region R2 is the plateau region where the electron density and ambipolar potential are nearly constant in space. Region R3 is the kinetic-stabilizer region of large stabilizing concave curvature.

the significantly lower electron temperature of the expander. The stand-off position may be determined at the point where the total stress tensor of the effluent matches the pressure of the kinetic-stabilizer beam. However, a proper theory for this intuitively-described model of the potential structure on either side of the abrupt stand-off region still remains for future work.

The characteristics of region R2 are determined by the kinetic-stabilizer beam. As has been discussed in section 2, in region R2, between the KS region and the stand-off point, a density plateau exists where the ambipolar potential and ion density are nearly spatially constant. This plateau region exists regardless of whether the KSTM beam is focused or unfocused; however, the plateau region has significantly higher density in the unfocused case.

We assume that the electrons in the kinetic stabilizer have a long mean-free-path and can be described by a Maxwellian distribution with temperature T_{eks}. For simplicity, we take $T_{eks} \ll m_i E_0$, although we stretch this inequality to its limits of validity. The Maxwellian assumption can be justified for the focused case where an ambipolar potential produces a dominant fraction of trapped electrons (shown in figure 6 in region R3 as a solid curve between $B_W < B < B_{ks}$); the majority of the electrons are trapped and confined long enough to relax by collisions to a Maxwellian distribution [5]. For the unfocused case, the determination of the mean electron energy in the R2 and R3 regions is far more complex. The electron distribution may not be a Maxwellian distribution in this case. For the unfocused case, the ambipolar potential monotonically increases to the wall values.

For the focused case, the schematic view of the ambipolar potential is shown in the region R3 of figure 6. This region is dominated by a large population of trapped electrons that neutralize the incoming ion beam but do not readily communicate with electrons in the central cell. The bulk of the electrons in the kinetic-stabilizer region are insulated from

the central-cell plasma by an ambipolar potential. The case with maximum MHD stabilization is particularly susceptible to the trapped particle instability [5].

The unfocused case leads to moderately reduced MHD stabilization, but has a far less restrictive condition for achieving trapped particle mode stabilization. Because the electrostatic potential monotonically increases in the direction from the expander towards the central cell, electrons with magnetic moment $\mu = 0$ feel an inwardly directed electrostatic force. However, electrons with a finite magnetic moment feel an outwardly directed mirror force that by itself would produce a magnetic trap what would prevent entrance to the central cell. Nevertheless, we presume that if any electron from the distribution of temperature $T_{\rm eks}$ penetrates through the stand-off point $B = B_{\rm st}$, it will also penetrate into the central cell because of the large electrostatic forces directed towards the central cell for $B > B_{\rm st}$. For this to happen $T_{\rm eks}B_{\rm mx}/B_{\rm st} < \kappa T_{\rm e0}$, where κ is a numerical constant of order unity. However the spatial potential profile is an important issue that may still prevent some electron penetration. For example, if most of the large potential drop is very close to the plug, a large fraction of the electrons would be reflected by the magnetic field and reduce the trapped electron penetration into the central cell. Nonetheless, we choose the most favourable case for satisfying the trapped particle instability: the case where all electrons that reach the abrupt stand-off section penetrate into the central region of the plasma.

Ions moving towards the central cell from the end wall do not have enough energy to penetrate beyond the stand-off region since the large ambipolar potential there repels them. These ions are blocked from penetrating by both the repulsive quality of the magnetic mirror force (accounted for in the distributions we have chosen) and ultimately by the extremely strong electrostatic force in the transition region that confines the hot central-cell electrons. In contrast, electrons in the kinetic-stabilizer region, whose source is from a supply originating from the end-walls, feel forces pushing them into the central cell. Hence, there are no confined ions sharing both the central cell and kinetic-stabilizer region. There are electrons that circulate both in the central cell and in the kinetic-stabilizer region. These electrons are a source for the charge uncovering term that is a stabilizing factor for the trapped particle mode [14].

The MHD stability criterion that we use in this paper strictly is the stability criterion for a low beta $m = 1$ flute mode where the radially perturbed displacement is constant everywhere along a cylindrical-like column and we shall apply this criterion to the finite beta regime. Consider a test function that pinches off the displacement so that there is zero displacement in the regions of favourable curvature. The trapped particle mode arises because the pinched-off potential removes the stabilizing influence from the good curvature region. In ideal MHD, the pinching process excites bending energy that allows the continued stabilization of the mode. However, kinetic processes enable the excitation of an electrostatic perturbation that does not excite bending energy. In addition, a low-beta flute mode is electrostatic, which enables relatively efficient coupling to other electrostatic perturbations. In a tokamak such coupling leads to the Kadomtsev–Pogutse trapped particle mode [15], which allows a curvature-driven instability to persist, but at a significantly reduced growth rate compared with the prediction from MHD theory. In a tokamak this reduced growth rate occurs due to the circulation of passing particles through the entire plasma. In a tandem mirror there is a substantially lower fraction of connecting particles than in a tokamak (where the fraction is near unity). Thus the relative growth rate of the trapped particle mode is larger relative to the trapped particle growth rate in a tokamak. When the fraction of trapped particles is sufficiently low and no additional stabilization mechanism is employed, the growth rate can even be as large as the MHD growth rate of the central cell and plugs. Mode stabilization of the trapped particle mode in a tandem mirror relies on the property that there can be a different fraction of connecting electrons to connecting ions. This difference leads to a stabilizing effect, which is considered below.

The stabilization condition for the $m = 1$ mode does not have the usual finite Larmor radius stabilization [16]. However, a similar stabilization mechanism arises due to *charge uncovering*, the difference between the number of electrons and ions that sample both the central cell and the kinetic-stabilizer regions. In ideal MHD, the cross-field currents due to the lowest order $\boldsymbol{E} \times \boldsymbol{B}$ drift do not produce an electrical current due to cancellation of electron and ion flow velocities. Because of finite Larmor radius effects, the ion $\boldsymbol{E} \times \boldsymbol{B}$ drift differs from the electron $\boldsymbol{E} \times \boldsymbol{B}$ drift. This leads to a current that produces charge accumulation. For trapped particle and for electrostatic modes, a similar current emerges due to the difference in electron and trapped ion particle populations.

We analyse the case where density and pressure profiles are Gaussian and have the form $R(z, \psi) = r(z) \exp[-\psi/2\psi_0]$ where $\psi = \psi(0) = B_0 r_0^2/2 = B(z)r^2(z)/2$. We follow past trapped particle mode studies in describing the electrons in the trapping region (in this work the KS region) by a Maxwellian distribution at a fixed temperature, $T_{\rm eks}$. Neglecting the effect of rotation found in their work, Berk and Lane [17] found the stability condition to be

$$\left(\omega_{\rm e}^* \Delta Q\right)^2 > 4\gamma_{\rm MHD}^2 (1 + Q), \tag{55}$$

where $\omega_{\rm e}^* = T_{\rm eks}/|e|B_0 r_0^2$. The square of the MHD growth rate $\gamma_{\rm MHD}^2$ is defined to be

$$\gamma_{\rm MHD}^2 = \frac{\int_{-L}^{L} {\rm d}z r_0^3(z) \frac{{\rm d}^2 r_0(z)}{{\rm d}z^2} \left(p_\perp(z) + p_{||}(z)\right)}{\int_{-L}^{L} {\rm d}z r_0^4(z) \rho_{\rm m}(z)}, \tag{56}$$

where $\rho_{\rm m}(z)$ is the mass density. Q is defined

$$Q = \frac{2\left(B_0 r_0^2\right)^2 \sum_j \int_{\rm ks} \frac{{\rm d}z}{T_j} r_0^2(z) n_{{\rm ct}j}(z) e_j^2}{\int_{-L}^{L} {\rm d}z r_0^4(z) \rho_{\rm m}(z)}, \tag{57}$$

and

$$\omega_{\rm e}^* \Delta Q = \frac{-2B_0 r_0^2 \sum_j \int_{\rm ks} {\rm d}z r_0^2(z) n_{\rm ct}(z) e_j}{\int_{-L}^{L} {\rm d}z r_0^4(z) \rho_{\rm m}(z)}, \tag{58}$$

where j denotes the species of particle with charge e_j. The density of particles of species j at position z that connect is

$n_{ctj}(z)$, i.e. these particles travel directly between the kinetic-stabilizer region and the central cell when a long mean-free-path electron limit is assumed.

In the kinetic-stabilizer region the eigenmode excitation is assumed to be negligibly small. The ambipolar sheath prevents ions outside the central region from returning to the central region, so that only electrons connect to the central cell. Thus in the expression for Q and ΔQ, only electrons contribute to the sums. For this case $\Delta Q = Q$, so that we find fulfilment of the trapped particle stability criterion requires

$$Q > 2\left(\frac{\gamma_{\rm MHD}}{\omega_{\rm e}^*}\right)^2\left(1+\sqrt{1+\left(\frac{\omega_{\rm e}^*}{\gamma_{\rm MHD}}\right)^2}\right) \underset{\left[\left(\frac{\omega_{\rm e}^*}{\gamma_{\rm MHD}}\right)^2\ll 1\right]}{\longrightarrow} 4\left(\frac{\gamma_{\rm MHD}}{\omega_{\rm e}^*}\right)^2. \tag{59}$$

If this condition is not met, the growth rate of the trapped particle mode is approximately given by [17]

$$\gamma_{\rm tp} \approx \gamma_{\rm MHD}/\sqrt{1+Q}. \tag{60}$$

If $Q < 1$ the intrinsic growth rate is purely MHD, as if no kinetic stabilizer were present.

For simplicity, as the stability condition for (59), we only use $Q > 4(\gamma_{\rm MHD}/\omega_{\rm e}^*)^2$ of (59), a *necessary condition* for the stability of the kinetic stabilizer to the trapped particle mode. In terms of physically intuitive parameters, the necessary stability condition is

$$T_{\rm eks}\int_{\rm ks} {\rm d}z r_0^2(z) n_{\rm ct}(z) > 4 \times \int_0^{L_{\rm c}+L_{\rm pl}} {\rm d}z\left(p_\perp(z)+p_\parallel(z)\right) r_0^3(z)\frac{{\rm d}^2 r_0(z)}{{\rm d}z^2}, \tag{61}$$

where ks refers to the z integration over a single kinetic-stabilizer region.

We investigate conditions that satisfy both MHD and trapped particle stability. To clarify the stability boundary we consider the MHD marginality parameter $M_{\rm ks}$ defined in (39). For an MHD stable system

$$M_{\rm ks} = \frac{\int_0^{L_{\rm c}+L_{\rm pl}} {\rm d}z\left(p_\perp+p_\parallel\right) r_0^3\frac{{\rm d}^2 r_0}{{\rm d}z^2}}{\int_{\rm ks} {\rm d}z\left(p_\perp+p_\parallel\right) r_0^3\frac{{\rm d}^2 r_0}{{\rm d}z^2}} < 1. \tag{62}$$

It is convenient to express the trapped particle stability condition relative to the MHD stabilization drive of the kinetic stabilizer as

$$\frac{T_{\rm eks}\int_{\rm ks} {\rm d}z r_0^2(z) n_{\rm ct}(z)}{4\int_0^{L_{\rm c}+L_{\rm pl}} {\rm d}z\left(p_\perp(z)+p_\parallel(z)\right) r_0^3\frac{{\rm d}^2 r_0}{{\rm d}z^2}} = \frac{T_{\rm eks}\lambda_{\rm k}\sigma_{\rm p}}{4 m_{\rm i} E_0 M_{\rm ks}}\left\langle\frac{n_{\rm ct}}{n}\right\rangle > 1. \tag{63}$$

In this expression, $\langle n_{\rm ct}/n\rangle$ is the fraction of electrons that have orbits in the kinetic stabilizer and also penetrate into the central cell. This fraction is

$$\left\langle\frac{n_{\rm ct}}{n}\right\rangle = \frac{\int_{\rm ks}\frac{{\rm d}z}{B} n_{\rm ct}(z)}{\int_{\rm ks}\frac{{\rm d}z}{B} n(z)}. \tag{64}$$

The numerical factor $\lambda_{\rm k}$ from the ratio in (63) is

$$\lambda_{\rm k} = \frac{\int_{\rm ks}{\rm d}z\int_0^1 \frac{{\rm d}x}{(1-x)^{1/2}}\frac{\left(\frac{\Delta\mu B}{E_0}\right)}{\left(x-\frac{B}{B_{\rm T}}\right)^2+\left(\frac{\Delta\mu B}{E_0}\right)^2}}{\int_{\rm ks}{\rm d}z\int_0^1 \frac{{\rm d}x}{(1-x)^{1/2}}(2-x)\frac{\left(\frac{\Delta\mu B}{E_0}\right)}{\left(x-\frac{B}{B_{\rm T}}\right)^2+\left(\frac{\Delta\mu B}{E_0}\right)^2}} \tag{65}$$

$$\cong \frac{\int_{\rm ks}{\rm d}z\frac{1}{\left(1-\frac{B}{B_{\rm T}}\right)^{1/2}}}{\int_{\rm ks}{\rm d}z\frac{2-\frac{B}{B_{\rm T}}}{\left(1-\frac{B}{B_{\rm T}}\right)^{1/2}}}. \tag{66}$$

The last approximate integral in (66) applies when the ion beams satisfy

$$\Delta\mu B_{\rm ks}/(E_0 - B/B_{\rm T}) \ll 1.$$

For beams with $\Delta\mu B_{\rm T}/E_0 \gg 1$, i.e. unfocused beams, we obtain $\lambda_{\rm k} \doteq 1/2$. For well-focused beams, where $B_{\rm T} = B_{\rm ks}$ and $\Delta\mu B_{\rm ks}/E_0 \ll 1$ we have $\lambda_{\rm k} \doteq 1$.

For a focused beam, the ion density build-up at $B \simeq B_{\rm T}$ allows for increased MHD stabilization of a factor of 1.5–3, as shown in figure 5. However, the focusing creates an ambipolar potential that prevents most of the electrons within the kinetic stabilizer from connecting to the central cell. For this reason the focused case may have the best MHD properties but is extremely susceptible to the trapped particle mode because the factor $\langle n_{\rm ct}/n\rangle$, the fraction of trapped and connecting electrons, is exponentially small.

We therefore examine the unfocused case which will have a substantially larger value of $\langle n_{\rm ct}/n\rangle$; for this case it may be possible to satisfy the trapped particle stabilization criterion. An unfocused beam results in $\lambda_{\rm k} \cong 0.5$ and the trapped particle stability criterion is

$$\left\langle\frac{n_{\rm ct}}{n}\right\rangle \frac{1}{8}\frac{T_{\rm eks}}{m_{\rm i}E_0} > M_{\rm ks}. \tag{67}$$

To apply this stability condition, we have calculated the normalized connecting particle electron density $n_{\rm ct}(z)/n(z)$

$$\frac{n_{\rm ct}(z)}{n(z)} = 1 - \sqrt{1-\frac{B(z)}{B_{\rm st}}}\exp\left[-\left(\frac{\psi_{\rm st}-\psi(z)}{\frac{B_{\rm st}}{B(z)}-1}\right)\right], \tag{68}$$

where $\psi(z) = -|e|\phi(z)/T_{\rm eks}$. The derivation of this formula is given in the appendix. Recall that the subscript st refers to the stand-off position. The connecting fraction of electrons $\langle n_{\rm ct}/n\rangle$, defined in (64), is evaluated numerically. The results of this calculation are shown in figure 7.

Despite an increase in the value of $\langle n_{\rm ct}/n\rangle$ compared with the trapped case, it is still difficult to satisfy the stability criterion given by (67) even when $M_{\rm ks}$ is substantially less than unity. This is because all factors on the left-hand side of (67) are relatively small. For example, in figure 7, $\langle n_{\rm ct}/n\rangle$ tends to be small, although it can be close to unity if the stand-off position can be made close to the inbound entrance to the kinetic-stabilizer region. Furthermore, if one attempts to raise the ratio $T_{\rm eks}/m_{\rm i}E_0$ to an order-unity quantity, the emerging ambipolar potential may prevent ion penetration into kinetic-stabilizer region. We find, in a calculation not discussed here [5], that when a self-consistent attempt to construct an ambipolar potential is made, raising $T_{\rm eks}/m_{\rm i}E_0 \approx 0.3$ leads

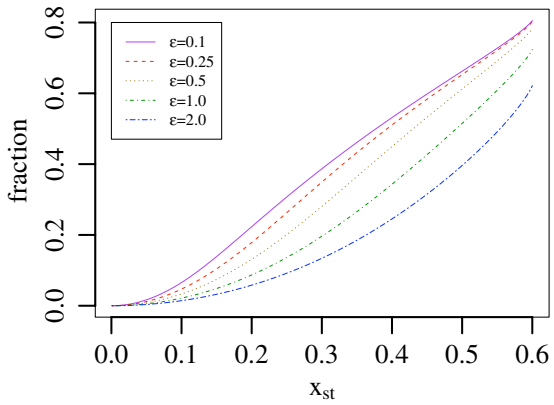

Figure 7. The connecting fraction of electrons in the kinetic-stabilizer region that reach the central cell. The relative radius of the kinetic-stabilizer entrance is $r_{ks}/r_W = 0.6$. The various curves are for different values of $\epsilon = \Delta\mu B_{ks}/E_0$. The connecting fraction is plotted as a function of the stand-off position $x_{ks} = r_{ks}/r_W$.

to a breakdown of the quasi-neutrality condition. Although higher electron temperature solutions should be possible with the formation of internal potential jumps on the order of a Debye length, it is likely that the maximum ratio $T_{eks}/m_i E_0$ that can give penetration of the ion beam into the kinetic stabilizer will remain below unity.

To satisfy the trapped particle stability criterion given by (67), we need to make the MHD stability margin parameter M_{ks} as small as possible; at the same time we must ensure that the largest acceptable kinetic-stabilizer beam power throughput is less than the alpha particle power production of the central cell. It then follows from (43) that M_{ks} lies in the interval

$$1 > M_{ks} > 70\frac{\lambda_c}{r_0(\mathrm{m})}\left(\frac{B_W}{B_0}E_0(\mathrm{keV})\right)^{1/2} \times\left(\frac{T_c(100\ \mathrm{keV})}{\beta_c}\right)\left(\frac{3}{B_0(\mathrm{T})}\right)^2. \quad (69)$$

We fold in the trapped particle stability criteria of (67) in with the MHD power constraint given in (43). For simultaneous stability to the MHD and trapped particle modes, as well as compatibility with the power restrictions of the kinetic-stabilizer beam, the kinetic-stabilizer's window is

$$\min\left[1, \left\langle\frac{n_{ct}}{n}\right\rangle\sigma_p\frac{T_{eks}}{8m_i E_0}\right] < M_{ks} \quad (70)$$
$$< 0.7\frac{\lambda_c}{r_0(\mathrm{m})}\left(\frac{B_W}{B_0}E_0(\mathrm{keV})\right)^{1/2}\left(\frac{T_c(100\ \mathrm{keV})}{\beta_c}\right)\left(\frac{3}{B_0(\mathrm{T})}\right)^2.$$

The trapped particle is always more restrictive than the MHD criterion. We take $\lambda_c = 0.175$, although design improvement from our nominal parameter choice can reduce λ_c. Hence the compatibility criterion becomes

$$4.6\frac{(\lambda_c/0.175)}{\sqrt{3}\,r_0(\mathrm{m})\sigma_p}\left(\frac{3B_W(\mathrm{g})}{B_0(\mathrm{T})E_0(\mathrm{keV})}\right)^{1/2}\left(\frac{T_c(100\ \mathrm{keV})}{\beta_c}\right) \times\left(\frac{3}{B_0(\mathrm{T})}\right)^2\left(\frac{m_i E_0}{2T_{eks}}\right)\left\langle\frac{n}{2.5n_{ct}}\right\rangle < 1. \quad (71)$$

We have arranged the left-hand side of (71), so that each of the bracketed terms have a nominal value of unity. We see difficulty in fulfilling this condition. Experimental designs that will allow the bracketed terms to achieve smaller values are needed. Much of the detailed physics is buried in the factor λ_c. For example, because λ_c is proportional to $1/\eta$, direct conversion of energy can reduce λ_c by an additional factor of five. Additional novel ideas could be developed to enable (71) to be satisfied. The nominal value of other factors, such as $(m_i E_0/2T_{eks})$ and $\langle n/2.5n_{ct}\rangle$, have been selected to have the smallest value we deemed possible. Hence, the present theory for a collisionless trapped particle mode indicates that there is a significant issue for the stabilization of a symmetric mirror machine with a kinetic stabilizer.

5. Summary and conclusions

We have investigated the compatibility of the kinetic stabilizer to both MHD stability and trapped particle stability. With sufficient kinetic-stabilizer beam input power, both MHD stability and trapped particle stability can be achieved. However the kinetic-stabilizer beam input power is limited because the power requirement for sustaining the kinetic-stabilizer beam must be substantially less than the fusion power being produced. Thus a window needs to be established in which sufficient beam power is provided to satisfy the MHD and trapped particle stability criteria and yet not violate the power input constraint imposed by the necessity of producing a power plant. Such a window is likely to be established from the power and MHD constraints alone. However, we find that it is significantly more difficult to satisfy the trapped particle stability criterion than the MHD stability criterion. The greater challenge to the kinetic-stabilizer concept is to be able to satisfy simultaneously both power constraints and stability to the trapped particle mode.

In our analysis the nominal maximum beam power is taken to be the fusion alpha power production, approximately 20% of the total fusion power production. The resulting MHD and power constraints lead to an allowable range of values for the MHD stability parameter M_{ks}, given by (52). A smaller value of M_{ks} improves stability and $M_{ks} = 1$ is the transition value between MHD instability and stability. The window of operation for simultaneous fulfilment of power requirements and trapped particle stability leads to the constraint (71). For the values chosen, the trapped particle instability criterion together with power constraints would not be satisfied in a burning plasma. Designs that could improve on our choices for the nominal parameters are needed. In the text we note that the parameter λ_c decreases substantially if direct conversion of the input beam power for the kinetic stabilizer is implemented. For example, if an 80% energy conversion efficiency could be achieved, the parameter λ_c reduces by a factor of 5. In this case the condition that both trapped particle stability and kinetic-stabilizer beam power input constraints are fulfilled, expressed by (71), is narrowly satisfied with all of the other parameters held fixed so that the parenthetic terms in (71) are unity.

A pertinent issue is how severe the trapped particle instability can be. A systematic experimental study of this instability has yet to be undertaken. In the kinetic-stabilizer region, if the electrons are in the short mean-free-path regime, the trapped particle instability growth rate is likely to decrease. Then it may be feasible to implement feedback techniques to prevent or reduce the harmful effects of the trapped particle

instability. Further studies, especially experimental studies, are needed to establish a database to assess the implications of exciting the trapped particle instability and determine whether the harmful effects of this instability can be mitigated.

Our study also indicates the need to develop systematic calculations for the ambipolar potential in the kinetic-stabilizer regime. The shape of the electric field in the case of unfocused beam propagation is particularly challenging to evaluate, because electrons in the kinetic stabilizer are in contact with the wall. In one transit, electrons are unlikely to be described by a Maxwellian distribution; it is necessary to verify how reasonable the model used in this work is for describing the potential structure in the KS region. A successful theory would enable the determination of the stand-off position, which separates the region where the ambipolar potential energy variation is characterized by the central-cell electron temperature from the region where it is characterized by the electron temperature.

There is an additional concern regarding the trapped particle stabilization criterion. If trapped particle stability is achieved by improving the communication of electrons from the kinetic-stabilizer beam to the central cell, there may be a break down in the thermal insulation of the hot electrons in the centre of the machine. Suppose a value of $\langle n_{ct}/n\rangle \sim 0.3$ is achieved, a reasonable estimate of the fraction of connecting electrons necessary to fulfil the trapped particle instability criterion. Then the current of cold electron entering the central cell will be 30% of the kinetic-stabilizer beam current. These connecting electrons are accelerated to the peak energy of the ambipolar potential and replace more energetic electrons that leave the system. The energy lost per electron in the exchange is comparable to the central-cell electron temperature. The thermal loss rate would be $\langle n_{ct}/n\rangle P_{ks}T_{ec}/E_0$, where T_{ec} is the electron temperature in the central cell and P_{ks} is the power sustaining the kinetic stabilizer. Since T_{ec} will be very large ($\geqslant 10^4$) the connection of the particles leads to an unacceptable power drain.

Another concern is that the local beta achieved by a focused kinetic-stabilizer beam may exceed unity. Such a plasma is formed by injecting a beam narrowly distributed in magnetic moment so that the beam will reflect back to the wall at designated target field position $B = B_{ks}$. At that position there is large favourable field-line curvature with the magnetic field designed so that $dr_{ks}/dz = 0$. Such a condition leads to a logarithmically large, stabilizing MHD response. Mixing the response of a focused beam with a completely unfocused beam may enable the best satisfaction of both MHD and trapped particle instability. The increase in the MHD response is logarithmic in the small parameter $\delta \equiv \sqrt{(\Delta r\Delta\mu)/(r_{ks}\mu_T)}$, where r_{ks} is the plasma field-line radius at $z = z_{ks}$ and Δr is the spread in the focusing position of the injected particle beam. The local beta increases as $\delta^{-1/2}$. Thus if significant MHD enhancement is achieved, the local beta value at B_{ks} is likely to be substantially larger than unity as has been discussed in section 3.4. An issue then arises regarding whether the desired focusing can be achieved.

Acknowledgments

Interesting discussions with Dimitry Ryutov, Richard Post and Wendell Horton are gratefully acknowledged.

Appendix. Calculation of the density of connecting electrons

We wish to derive an expression for the density of connecting electrons, $n_{ct}(z)$. The electrons are assumed to have Maxwellian distribution of the form

$$f\left(v^2\right) = \frac{1}{\sqrt{2\pi}}\exp\left[\psi(z) - \left(\frac{v_\perp^2}{2} + \frac{v_\parallel^2}{2}\right)\right], \tag{A.1}$$

where the normalization had been chosen so that the electron kinetic energy and ion potential energy ψ are in units of T_{eks}/m_e and that local density is

$$n(z) = n_W\int_{-\infty}^{\infty} dv_\parallel \int_0^\infty dv_\perp v_\perp f\left(v^2\right) = n_W\exp\left[\psi(z)\right]. \tag{A.2}$$

The connecting particles are those that reach the stand-off position $z = z_{st}$ with a non-zero $v_{||}$. It follows from energy conservation and magnetic moment conservation that the connecting particles satisfy the condition

$$\frac{v_\perp^2}{2} + \frac{v_\parallel^2}{2} - \psi(z) \geqslant \frac{v_\perp^2 B_{st}}{2B(z)} - \psi_{st}. \tag{A.3}$$

Thus

$$v_\perp^2 \leqslant \frac{v_\parallel^2 + 2\left[\psi\left(z_{st}\right) - \psi(z)\right]}{\frac{B_{st}}{B(z)} - 1} \equiv v_{\perp mx}^2(v_\parallel). \tag{A.4}$$

The connecting density is then evaluated by integrating over the electron Maxwellian distribution inside the kinetic stabilizer with the inequality given by (A.4) satisfied.

$$n_{ct}(z) = n_W\int_{-\infty}^{\infty}\frac{dv_\parallel}{\sqrt{2\pi}}\exp\left(-\frac{v_\parallel^2}{2}\right) \times \int_0^{v_{\perp mx}^2(v_\parallel)}\frac{dv_\perp^2}{2}\exp\left(-\frac{v_\perp^2}{2} + \psi(z)\right), \tag{A.5}$$

$$= n(z)\left(1 - \int_{-\infty}^{\infty}\frac{dv_\parallel}{\sqrt{2\pi}} \times \exp\left[-\frac{v_\parallel^2}{2}\frac{\left[B_{st} + (\psi_{st} - \psi(z))\,B(z)\right]}{B_{st} - B(z)}\right]\right), \tag{A.6}$$

$$= n(z)\left(1 - \left(\frac{B_{st} - B(z)}{B_{st}}\right)^{1/2} \times \exp\left[-\frac{(\psi_{st} - \psi(z))\,B(z)}{B_{st} - B(z)}\right]\right). \tag{A.7}$$

References

[1] Rosenbluth M.N. and Longmire C.L. 1957 *Ann. Phys.* **1** 120–40
[2] Post R.S., Brau K., Casey J. and Coleman J. 1988 *MIT Plasma Fusion Center Report* PFC/JA-88-34
[3] Molvik A.W. *et al* 1981 MHD stability experiments in the phaedrus tandem mirror *American Physical Society 23rd Annual Meeting (New York, 12–16 October 1981)*
[4] Molvik A.W. *et al* 1982 *Phys. Rev. Lett.* **48** 742–5
[5] Pratt J. 2009 Drift wave stability and transport in tandem mirrors *PhD Thesis* University of Texas at Austin

[6] Post R.F. 2007 The kinetic stabilizer; a route to simpler tandem-mirror systems? *Proc. 4th Symp. on Current Trends in International Fusion Research (Washington, DC, 2001)* (Ottawa, Ontario: NRC Research Press) p 291
[7] Nagornyj V.P., Ryutov D.D. and Stupakov G.V. 1984 *Nucl. Fusion* **24** 1421
[8] Ryutov D.D. 1987 Axisymmetric MHD-stable mirrors *Physics of Alternative Magnetic Confinement Schemes* vol 2 (Varenna: Societa Italiana di Fisica) pp 791–816
[9] Anikeev A.V. *et al* 1997 *Phys. Plasma* **4** 347
[10] Ivanov A.A. 1991 *Physics of Alternative Magnetic Confinement Schemes* ed S. Ortolani and E. Sindon (Varenna: Societa Italiana di Fisica) pp 443–58
[11] Moir R.W. and Barr W.L. 1973 *Nucl. Fusion* **13** 35
[12] Krall N.A. 1966 *Phys. Fluids* **9** 820–1
[13] Breizman B.N., Tushentsov M.R. and Arefiev A.V. 2008 *Phys. Plasmas* **15** 057103
[14] Berk H.L., Rosenbluth M.N., Wong H.V., Antonsen T.M. and Baldwin D.E. 1983 *Sov. J. Plasma Phys.* **9** 108
[15] Kadomtsev B.B. and Pogutse O.P. 1971 *Nucl. Fusion* **11** 67–92
[16] Rosenbluth M.N., Krall N.A. and Rostoker N. 1962 *Nucl. Fusion* **2** (Suppl.) 143–50
[17] Berk H.L. and Lane B.G. 1986 *Phys. Fluids* **29** 3749–59